

Spike timing amplifies the effect of electric fields on neurons: implications for endogenous field-effects

Thomas Radman, Yuzhuo Su, Je Hi An, Lucas C. Parra^{*}, Marom Bikson^{*}

Department of Biomedical Engineering, City College of the City University of New York, New York, NY 10031

Despite compelling phenomenological evidence that small electric fields (<5 mV/mm) can affect brain function, a quantitative and experimentally verified theory is currently lacking. Here we demonstrate a novel mechanism by which the non-linear properties of single neurons 'amplify' the effect of small electric fields: when concurrent to supra-threshold synaptic input, small electric fields can have significant effects on spike timing. For low-frequency fields our theory predicts a linear dependency of spike timing changes on field strength. For high-frequency fields (relative to the synaptic input), the theory predicts coherent firing; with mean firing phase and coherence each increasing monotonically with field strength. Importantly, in both cases, the effects of fields on spike timing are amplified with decreasing synaptic input slope and increased cell susceptibility (mV membrane polarization per field amplitude). We confirmed these predictions experimentally using CA1 hippocampal neurons *in vitro* exposed to static (DC) and oscillating (AC) uniform electric fields. In addition, we develop a robust method to quantify cell susceptibility using spike timing. Our results provide a precise mechanism for a functional role of endogenous field oscillations (e.g. gamma) in brain function, and introduce a framework for considering the effects of environmental fields and design of low-intensity therapeutic neuro-stimulation technologies.

Introduction

The study of how small electric fields affect brain function is important for several reasons. First, these studies provide insight into the mechanisms by which endogenous electric fields generated by the brain itself (e.g. delta, theta, gamma) could 'feed-back' unto the brain (Lutz et al. 2001, Parra and Bikson, 2004; Schaefer et al., 2006). Second, these studies address concerns about human exposure to environmental electromagnetic fields (Hamblin 2002; Jefferys et al. 2003). Lastly, they have practical applications in the design of low-intensity brain stimulation treatments for neurological diseases (Ghai et al., 2000; Francis et al., 2003; Webster et al., 2006).

Small electric fields will polarize neurons by only a small amount; for this reason small electric fields have previously been suggested to have no physiologically relevant effects. However, the hypothesis that small fields can affect brain function has garnered support from phenomenological studies applying low-intensity electrical stimulation to brain slices (Ghai et al., 2000; Francis et al., 2003; Bikson et al., 2004) and humans (Marshall et al., 2006; Webster et al., 2006), the latter indeed showing a causal effect on slow wave oscillations and declarative memory. A quantitative and experimentally verified explanation for these findings has previously been lacking.

While neurons often encode information in their firing rate, the timing of individual action potentials (temporal coding) has also been shown to carry significant information (de Ruyter et al., 1997). Cortical neurons have been identified that fire with an accuracy of a few milliseconds in response to sensory stimuli (Mainen and Sejnowski, 1996; Trussel, 1999; Kara et al. 2000; Reinagel and Reid, 2000; DeWeese et al., 2003), in synchrony with overt behavior (Riehle et al., 2000), and in phase with ongoing *extracellular potential* oscillations (Kashiwandi et al., 1999; Mehta et al., 2002; Harris et al., 2003).

Here we consider how small electric fields, which are in themselves not sufficient to trigger or suppress action potential activation in response to synaptic input, may nonetheless have an effect on neuronal information processing through induced changes in spike *timing*. Specifically, given a steady firing threshold and knowing that a membrane polarizes linearly with field strength (where the proportionality constant represents the susceptibility of the membrane potential to extracellular fields; Bikson et al., 2004), we make a number of quantitative predictions on the effects of extracellular fields on a neuron's spike timing: (1) For relatively low-frequency or DC fields, spike timing advances linearly with increasingly depolarizing field strength; (2) Oscillating fields promote coherent firing with the mean phase of firing falling within < 1/4 of the oscillatory cycle (on the positive rising edge); (3) Time advancement, phase delay, and coherence strength all increase with field strength amplified by membrane susceptibility and the inverse synaptic ramp slope. These quantitative predictions are validated here for hippocampal CA1 neurons *in vitro*. In addition, we develop a method to determine membrane susceptibility based on spike timing measurements. Taken together, this work yields the first quantitative framework for evaluating the effect of sub-threshold fields, with arbitrary (non-uniform) spatio-temporal waveform, on neuronal spike timing.

Methods

Transverse hippocampal slices (350 μ m) were prepared from male Sprague-Dawley rats (125–150 g); anaesthetized with intraperitoneal ketamine (7.4 mg kg⁻¹) and xylazine (0.7 mg kg⁻¹) and killed by cervical dislocation. The slices were stored in a holding chamber submerged in artificial cerebrospinal fluid (ACSF) consisting of (mM): 125 NaCl, 26 NaHCO₃, 3 KCl, 1.6 CaCl₂, 1.5 MgSO₄, 1.25 NaH₂PO₄, and 10 glucose, bubbled with a mixture of 95% O₂–5% CO₂. After >60 min, slices were transferred to an interface recording chamber at 33°C.

Uniform electric fields were generated across individual

^{*} both authors contributed equally to this work.

Correspondence should be addressed to bikson@ccny.cuny.edu

Accepted Feb. 12, 2007

slices by passing current between two parallel Ag/AgCl electrodes (Ghai et al., 2000; Bikson et al., 2004) placed on the surface of the ACSF in the interface chamber; the wires were parallel to the direction of perfusate flow, 12 mm long and 10 mm apart. Field intensities were generated by a Power 1401 ADC/DAC (Cambridge Electronic Design, Cambridge, UK) and converted to a constant current by a stimulus isolation unit (2200, A-M Systems, Carlsborg, WA, USA). The electric field (mV/mm or $\text{mV}\cdot\text{mm}^{-1}$) in the chamber was measured by two recording electrodes separated by 1 mm and calibrated to the current passed through the Ag–AgCl electrodes (Ghai et al., 2000; Durand and Bikson, 2001; Bikson et al., 2004); the polarity convention used refers to the anode on the Alveus side of the hippocampus.

Conventional recording techniques were used to measure activity from the CA1 pyramidal cell region. Intracellular electrodes (40–120 M Ω , pulled on a P-97; Sutter Instruments, Novato, CA, USA) were filled with 3M potassium chloride. Pyramidal neurons with an input resistance > 15.4 M Ω , resting membrane potential < -53.5 mV, over-shooting action potentials, and no spontaneous action potentials were accepted. Cell input resistance was monitored with a -0.3 nA current step. The voltage recorded by a field electrode (placed within 50 μm of the impaled neuron) was subtracted from the intracellular potential to obtain the transmembrane voltage and (partially) compensate for the exogenous potential artifact. For DC electric field experiments, no holding current was used. For AC electric field experiments, holding current (< -0.3 nA) was modulated to stabilize the resting membrane potential (RMP).

Depolarizing intracellular current ramps (0.1–1.6 nA/s) were generated and triggered to halt <100 ms after action potential detection. The initiation of subsequent current ramps was intercalated by an eight second delay. The experimental paradigm consisted of interlacing control (no field) ramp trials with ramps applied during field application. Extracellular field application was initiated 400 ms before activation of depolarizing intracellular current ramps. Alternate DC polarity fields or alternate 30 Hz AC fields shifted 1/60 ms (180°) were tested, at varied peak field strengths (mV/mm). AC stimulation also included interleaved DC field and control trials as required to determine membrane susceptibility (see results). Signals were subtracted, amplified, and low-pass filtered (1–10 kHz) with an Axoclamp-2B (Axon Instruments, Union City, CA, USA) and FLA-01 amplifiers (Cygnus Technology, Delaware Water Gap, PA, USA); then digitized and processed using a Power 1401 and Signal software (CED).

Unless otherwise stated, all results are reported as means \pm S.D.; n = number of cells. For resolution of lower-limit (<5 mV/mm) DC field effects, a paired t-test was performed for each cell at a single field magnitude by averaging time to first spike of neighboring control trials and pairing this with interlaced field trials (i.e. control / field / control), positive and negative fields were grouped due to field-effect symmetry resulting in 44–160 trials per neuron. For AC fields, phase-shifted trials of a single magnitude were combined (by subtracting 180° from one) resulting in 11–164 trials per neuron and field condition. The phase of the first spike relative to the applied field was determined. Mean firing phase, Φ , and vector strength, r , were computed from the population vector, which is defined as, $\vec{r} = \int d\varphi p(\varphi) \vec{r}_0(\varphi)$, with $\vec{r}_0(\varphi) = [\cos \varphi, \sin \varphi]$, and $p(\varphi)$ is the distribution of phases. This population vector can be estimated

from the observed phases φ_i as the sample average, $\vec{r} = \frac{1}{N} \sum_{i=1}^N \vec{r}_0(\varphi_i)$. Linear regression was used to model the dependence of mean phase and coherence on field strength coefficient. Residuals from the regression line were used as criterion for outlier rejection based on inter-quartile range. (Moore et al., 1999).

Results

The single neuron amplification mechanism was validated using hippocampal CA1 pyramidal neurons *in vitro*. We first confirmed that firing time in response to injected depolarizing current ramps varies linearly with incremental polarization and in proportion to the inverse of ramp slope. We then demonstrated that timing changes in direct response to applied uniform DC fields follow the same linear properties. These timing changes were used to derive membrane polarization susceptibility. Finally, we confirmed the predicated effects of AC fields (in the gamma frequency range) on firing coherence and phase. Portions of this work have been previously presented in preliminary form (Radman et al., 2006).

Firing time changes linearly with increasing polarization

Assuming a constant firing threshold one would expect that an incremental polarization ΔV , which is applied with a voltage ramp, $\dot{V} = dV/dt$, should lead to a time advancement of: $\Delta t = \Delta V / \dot{V}$, where Δt is the firing time of control minus the field stimulus condition. Hyper-polarization of CA1 pyramidal neurons, with an increasingly negative DC holding current, ΔI , incrementally delayed action potential firing time in response to an intracellular current ramp, \dot{I} . (Linear current ramps lead to linear voltage ramps if the change is sufficiently slow – here 0.1–1.6 nA/s). Importantly, for the conditions tested here, action potential threshold did not vary with ramp slope or polarization in agreement with previous findings (Fricker et al., 1999). The change in timing increased linearly with the holding current, and inversely proportional to ramp slope (Fig. 1; n=12 cells, $r^2 > 0.95$ for linear regressions). These results show that the membrane dynamics of real CA1 pyramidal neurons support the single neuron amplification mechanism hypothesized (R is membrane resistance):

$$\Delta t = \frac{\Delta I}{\dot{I}} = \frac{R \Delta I}{R \dot{I}} = \frac{\Delta V}{\dot{V}} \quad (\text{Eq. 1})$$

Spike time advances with increasing applied DC electric fields

Uniform DC electric fields were generated across hippocampal slices while synaptic input was simulated by injecting a current ramp. Constant uniform fields induced a membrane polarization; consistent with previous reports (Chan et al., 1986; Bikson et al., 2004), the magnitude of the somatic polarization was a linear function of field strength and the polarity was dependent on the direction of the field (not shown). Applied fields could significantly modulate the firing latency of single neurons resulting from intracellular depolarizing ramp current injection. DC fields inducing membrane hyperpolarization delayed action potential initiation while fields inducing membrane

depolarization had the opposite effect (Fig. 2A; $n=8$). For each injected ramp slope, the experimental data could be fit with a regression line ($r^2 = 0.90 \pm .1$); the slope of this fit indicated the change in timing induced per mV/mm applied electric field (in s/mV \cdot mm $^{-1}$). As intracellular ramp slope decreased, the fit timing sensitivity to applied fields (s/ mV \cdot mm $^{-1}$) linearly increased, supporting our prediction of an inverse relationship. This inverse relationship is summarized for 3 cells in Figure 2B where for each cell the changes in time per electric field ($\Delta t/E$) is plotted against the corresponding injected ramp slope (\dot{V}).

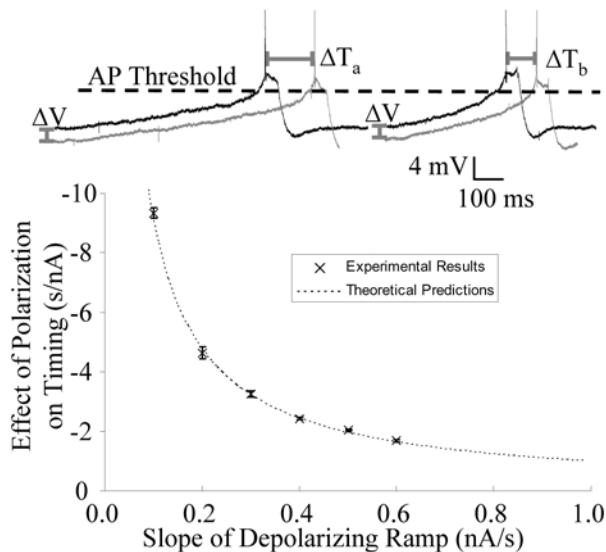


Figure 1. CA1 pyramidal cell response to depolarizing current ramps. **Top:** Intracellular recording of the response to a 0.4 nA/s (left) and 0.7 nA/s (right) intracellular current ramp (action potentials clipped). In both cases hyperpolarization (ΔV) delayed the AP firing time. The change (ΔT), is inversely proportional to depolarizing ramp slope, $\Delta T_a:\Delta T_b$ as 1/0.4:1/0.7. **Bottom:** The inverse relationship between the ramp slope and the sensitivity to membrane polarization due to negative DC holding current can be summarized in a single plot. Experimental results (“x”) fit directly to the theoretical prediction of an inverse slope. Error bars represent standard error of the slope of a linear regression line fitting holding current (nA) versus AP timing (s) data ($n \geq 7$ for linear regression data).

The somatic polarization induced by an electric field is set by the cell-specific membrane susceptibility constant c , $\Delta V=cE$. Membrane susceptibility can be determined using timing data by extension of (Eq. 1): $c = \dot{V}\Delta t/E$ (see also Eq. 2 in discussion). Susceptibility may thus be calculated from a single timing change measurement at one field amplitude, using a single intracellular ramp slope. A more robust method involves using the inverse relationship in Fig 2B to simultaneously fit all data from a single cell. Indeed, for each cell, these plots are well approximated by the curve, $y = cx^{-1}$, ($r^2 > 0.98$, $y = \Delta t/E$, $x = \dot{V}$) where c indicates the estimated membrane susceptibility. Using this indicator, we determined polarization susceptibilities of $c = 0.11 \pm 0.05$ mV/mV \cdot mm $^{-1}$ ($n=10$). Using a conventional method (Bikson et al., 2004) consisting of recording the intracellular potential and subtracting the measured stimulation

‘artifact’ at a second iso-potential electrode, the polarization induced per electric field was 0.13 ± 0.14 mV/mV \cdot mm $^{-1}$ ($n = 9$).

Resolution of lower-limit DC effects

For a 0.4 nA/s injected current ramp, we observed a significant change in timing induced by ± 1 mV/mm DC field strengths ($n = 4$). The average change in timing observed was 11 ± 5 ms (mean \pm SEM). Assuming a susceptibility of 0.11 mV per 1 mV/mm applied field and a 12 mV/s voltage ramp (induced by a 0.4 nA/s current injection into an ~ 30 M Ω cell resistance), a change in timing of ~ 9 ms would be expected.

For 0.5 mV/mm DC fields and a 0.4 nA/s current ramp, a statistically significant change in timing was observed in 1 of 4 neurons tested. For the cell showing a significant change, the average change in timing observed was 8 ± 3 ms (mean \pm SEM), while 4.5 ms was the predicted change (as above).

In attempts to resolve significant timing changes due to .5 mV/mm DC electric fields, we could reject the null hypothesis of a sample mean different than zero in 1 out of 4 attempts. For our experimental paradigm, the standard deviation of the difference between time to action potential under a 0.5 mV/mm field and a control trial was 54 ms for 0.4 nA/s current injections. If this standard deviation remained stable over time, we would need > 500 tests to resolve the predicted 4.5 ms difference induced by a 0.5 mV/mm field in 50% of neurons tested. Conversely, our attempts to resolve the effects of .5 mV/mm fields with < 160 trials leads to a power of a $< 80\%$ chance to reject an effect when it is really there (Type II, β error); indeed, we rejected 75% of our attempts. For the predicted timing change in response to a 1 mV/mm field, we would expect to detect a significant change in 83% of our attempts (< 160 trials); we resolved all four neurons. We note that the limits to resolve a field-induced change are determined by the noise (experimental and biological) in spike timing and subsequent effect on the repeats necessary to reach statistical significance; the latter is limited by duration of neuronal impairment integrity.

Uniform AC electric fields induce spike coherence

Uniform AC electric fields were generated across hippocampal slices and the firing time in response to an intracellular depolarizing ramp monitored. The frequency (30 Hz) and slope of the ramp (72 ± 22 mV/s) were selected to mimic extracellular gamma oscillations and synaptic theta depolarization (Harris et al., 2002) typical for theta-modulated gamma activity (Chrobak et al., 2000, Fischer et al., 2002). Significant coherence of the firing time with the applied field oscillation was observed in 21 of 29 field conditions (Rayleigh test, $p < 0.02$) including fields as low as 1mV/mm. Mean firing phase was analyzed for 19 field conditions (excluding two outliers, see methods). During application of fields, neuron coherence (as measured by the Rayleigh vector strength) increased with the mean firing phase falling approximately within 1/4 of the oscillatory cycle ($40^\circ - 110^\circ$, Fig. 3). For each cell, the coherence and mean phase were plotted against the field amplitude applied to that cell (in mV/mm) times the individual cell susceptibility (determined as above using interleaved DC stimulation trials) and divided by the current-induced voltage ramp slope and field period (i.e. $cE(\dot{V}T)^{-1}$; see discussion); the resulting plots (Figure 3C) show significant correlation with this characteristic parameter (phase, $p < 0.02$; coherence, $p < 0.002$).

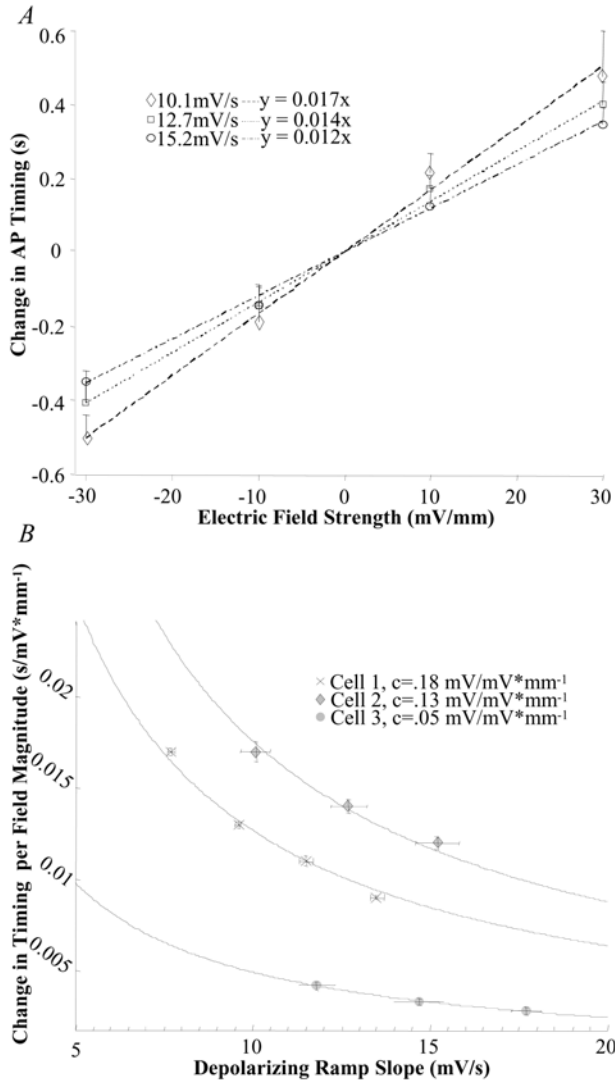


Figure 2. Effects of applied extracellular DC electric fields on CA1 pyramidal neuron firing time in response to intracellular depolarizing ramp slopes. **A**, Positive (hyper-polarizing) fields delayed action potential initiation while negative (depolarizing) fields expedited AP onset. Note that for each ramp slope series, the relationship between firing time (Δt) and applied field amplitude is linear. Moreover, the slope of this relationship varies inversely with the slope of the injected intracellular ramp (i.e. 10.1:12.7:15.2 as 1/.017:1/.014:1/.012). The injected current ramp slope (.4, .5, .6 nA/s) translated to voltage slope by cell resistance (25.3 M Ω for this cell). The change in timing for any given field is 'amplified' as the slope of the ramp is decreased. Reported: mean \pm SD ($r^2 > .94$, $p < .01$ for the three regressions shown here). **B**, The relationship between ramp slope and timing change per field magnitude is plotted for 3 cells. Each line in Fig. 2A corresponds to a point of the "Cell 3" series shown (vertical error bars show standard error of the slope, horizontal show SEM). Data for each cell is fit with $y=c/x$ ($r^2 > .98$, $p < .01$ for all regressions shown). Legend shows membrane susceptibility, c , in units of $\text{mV}/\text{mV}\cdot\text{mm}^{-1}$ ($y\cdot x$ or $\text{s}/\text{mv}\cdot\text{mm}^{-1}\cdot\text{mV}/\text{s}$).

Discussion

Predictions of timing changes

Despite mounting phenomenological evidence that small fields

can entrain network activity, and have an effect on brain function, to date, there is no experimentally verified mechanistic theory on how this causal interaction may occur. We hypothesized that incremental polarization due to an extracellular field will affect the time of threshold crossing; under the assumption of a constant firing threshold we made a number of predictions that will now be described.

For the case of low-frequency or DC extracellular fields with strength E , which polarize a cell by, $\Delta V_E = cE$, where c is the susceptibility of the membrane to an extracellular field, we predicted an advance in spike timing of:

$$\Delta t = \frac{\Delta V_E}{\dot{V}_I} = \frac{cE}{\dot{V}_I} \quad (\text{Eq. 2})$$

Note that c refers to the susceptibility effective at the site of spike initiation (i.e. the soma). Subscripts emphasize that ΔV_E results from application of the extracellular field, while \dot{V}_I is the result of a concurrent intracellular/synaptic current ramp which induces the action potential spike.

For the case of AC fields, we predicted increased coherence of spiking with the ongoing oscillations. Change in coherence can be quantified as a change in the distribution of firing times occurring at phase φ within the oscillatory cycle (with duration T). The distribution of firing phase, $p(\varphi)$, for the present experimental preparation can be expressed as:

$$p(\varphi) \propto \frac{1}{2\pi} + \frac{1}{T} \frac{cE}{\dot{V}_I} \cos(\varphi + \alpha) \quad (\text{Eq. 3})$$

assuming that φ is within a depolarizing phase of the membrane oscillation, and the cell has not yet fired (green shaded region in Fig. 3B), otherwise, $p(\varphi) = 0$, since only the time to the first spike was analyzed in the experiment (red shaded region). Eq. 3 assumes a uniform initial distribution and no noise (see supplementary material for derivation). Because the membrane acts as a low pass-filter, a delay between the extracellular field and the induced transmembrane polarization phase is expected; this is expressed in Eq. 3 as phase delay, α . The phase distribution of Eq. 3 can be characterized by the mean phase, Φ , and the vector strength, r , as shown in Fig. 3C. Both should increase monotonically with cE/\dot{V}_I , with mean phase remaining constrained to the range, $\alpha \leq \Phi \leq \alpha + 90^\circ$ (see Fig. S1).

This series of predictions were born out under the experimental conditions tested.

For both, DC and AC fields, the strength of the effect on spike timing scales with:

$$\frac{cE}{\dot{V}_I} = GE \quad (\text{Eq. 4})$$

where, $G = c/\dot{V}_I$, can be considered as a timing amplification factor. It increases with the susceptibility of the membrane to extracellular polarization (mV of transmembrane polarization at the site of action potential initiation per mV/mm extracellular field) and decreases with the depolarizing synaptic ramp slope

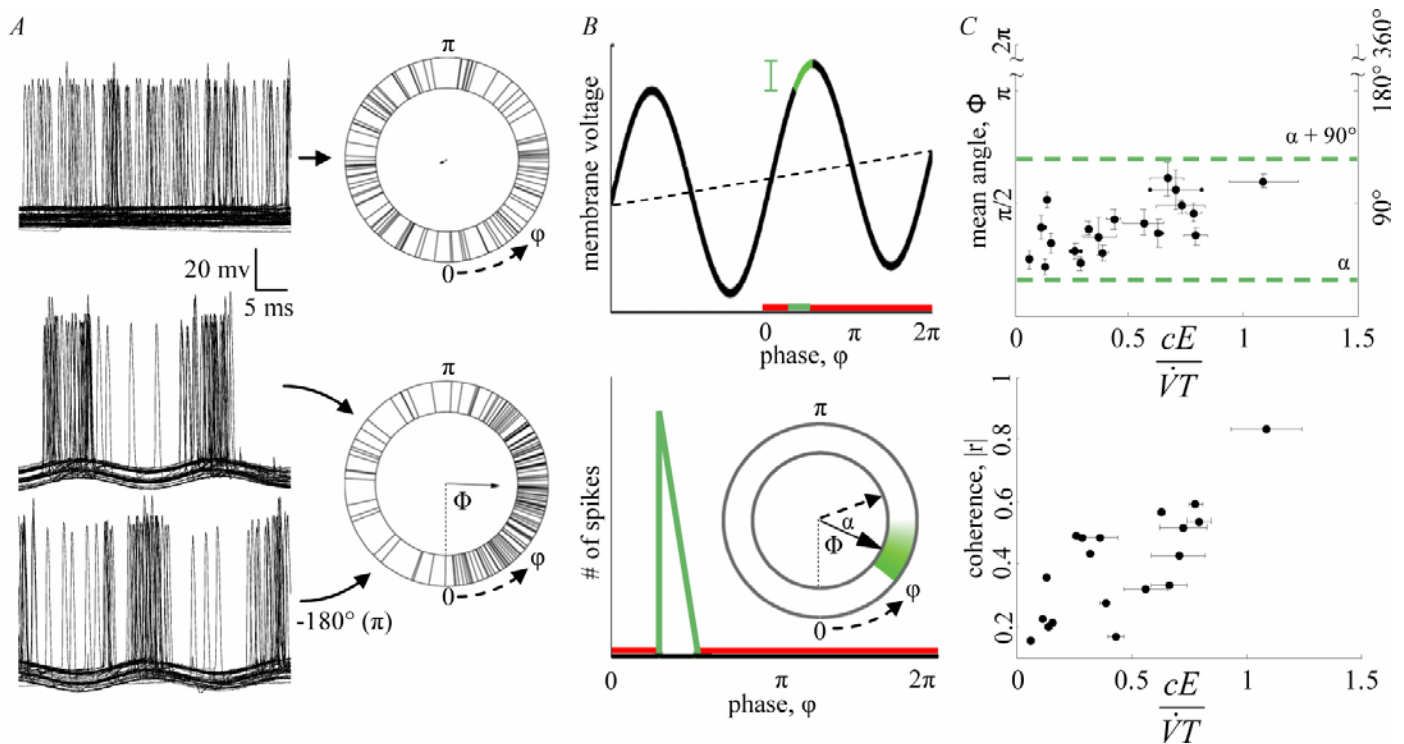


Figure 3. Effects of applied extracellular AC electric fields on CA1 pyramidal neuron firing time in response to intracellular depolarizing ramp slope. **A**, Overdrawn intracellular recordings in response to an injected current ramp with accompanying circular scatter plot. Top traces and circular plot: in the absence of uniform AC electric field (control), spike traces show low coherence and insignificant (random) mean angle. For circular scatter plots, outer edge shows individual spike phase ϕ , direction of arrow on inset shows mean angle, Φ , length of arrow shows coherence as measured by vector strength, r , with perfect coherence reaching edge of inset. Lower traces and plot: middle trace shows overdrawn samples in the presence of a 10 mV/mm uniform 30 Hz AC electric field (stimulus), bottom trace in the presence of a 10 mV/mm uniform 30 Hz AC electric field phase shifted 180 degrees from previous (stimulus). Lower circular scatter plot combining field-present cases (by shifting data of bottom-left case back 180 degrees), arrow shows increased coherence with a mean firing phase at $\sim\pi/2$, on the rising edge of electric field oscillation. **B**, Theoretical predictions of AP phase response to injected current ramp under AC electric field. Top: dashed line shows simulated membrane voltage with same control condition as in experiment “A”. Black trace shows the simulated membrane response under field stimulus condition as in “A”. If the previous cycle did not cross threshold, the membrane will not increase to a greater value during the red region on the phase axis. The cell is thus constrained to fire in the “unvisited” voltages (green), in this case on the positive rising field edge quadrant ($<\pi/2$). Bottom: predicted distribution of spike timing phase; the inset shows the resulting circular plot of this distribution with mean angle and vector strength. Assuming a delay, α , between the extracellular field and induced membrane polarization, the dashed arrow shows the mean firing phase relative to the extracellular field; note similarity to experimental results in “A”. **C**, Experimental results of mean phase and coherence vector strength. Horizontal axes is given by the experimentally observed value of (see discussion). The dashed green lines indicate the field positive rising edge quadrant shifted by an estimated $\alpha = 40^\circ$ membrane phase delay (see discussion). Error bars show SEM.

(in mV/s). For the case of AC fields, the timing amplification factor is further scaled by field frequency ($1/T$).

Generalization and Quantitative parameterization

Equations 2 through 4 provide a general theoretical framework for considering the effects of any electric field on spike timing in any neuron with appropriate membrane dynamics (see below). Quantitative application requires knowledge of the intracellular (ramp slope) and extracellular (field amplitude and period) waveforms, which are readily measured. For low-frequency (quasi-static) fields, cell susceptibility can be determined using the method outlined above.

Equation 3 can be readily applied to any periodic field with a complex spatio-temporal profile, by considering only the maximum positive instantaneous cE (the phase in the field cycle when the induced transmembrane depolarization is maximal). The susceptibility, c , is specific to a given spatio-temporal waveform (e.g. frequency, non-uniformity). The uniform field

susceptibility, for any given temporal waveform, presumably sets a *lower* susceptibility bound for non-uniform fields. The membrane, acting as a low-pass field filter (Bikson et al., 2004), may introduce a frequency-specific phase delay $\alpha > 0^\circ$, as well as an attenuated (relative to DC) susceptibility. The DC field susceptibility thus sets an upper limit for AC fields of *comparable spatial profile*. The phase delay may be estimated assuming the membrane acts as a first-order low pass filter; thus a membrane time constant of $\tau = 30$ ms should result in a phase delay of $\alpha \approx 40^\circ$ for 30 Hz fields, consistent with our experimental findings using timing data (Fig. 3).

Applying timing changes to discern susceptibility

As reinforced above, the polarization susceptibility of neurons is of fundamental importance in assessing subsequent effects on nervous system function. The field induced polarization is inherently variable between neurons due in part to alignment with the field, neuronal geometry, and membrane biophysical

properties (Rattay, 1998). Here we developed a method utilizing measured timing changes, to calculate the sensitivity of the neuron to polarization by an electric field (Fig. 2B). This technique may yield greater accuracy in measuring polarization sensitivity to small (<5 mV/mm) electric fields than can be achieved by conventional methods. Conventional methods are limited because experimental (line) noise is of magnitude comparable to the polarization induced by small fields and they require an additional, precisely positioned, iso-potential field electrode. Our timing-based method may be readily applied for non-uniform fields (e.g. unipolar, bipolar, DBS spatial waveforms) and *in vivo*. As a further advantage, our timing method may inherently extract the susceptibility at the spike initiation zone. Conventional polarization measurements here and previously (Bikson et al., 2004), show average susceptibility (coupling-constant) values similar to our method utilizing timing changes.

Membrane Dynamics and Noise

The theory developed here assumes a simple threshold mechanism equivalent to an integrate-and-fire model neuron with constant firing threshold. The accuracy of the assumption of constant threshold depends on a number of factors including the channel kinetics of the specific cell type and the nature of the incoming synaptic input; experimental and theoretical work show both dynamic and constant thresholds (Fricker et al. 1999; Azous and Gray 2000). The present experiments with DC stimulation controlled for potential slope-dependent thresholds by measuring only changes in timing relative to a control condition with the same ramp slope. The experimental data for the AC stimulation is generally consistent with a constant threshold.

Interestingly, our theory on the scaling of timing effects with ramp slope also explains a number of existing observations on the timing jitter that results from synaptic and membrane noise. If noise induces variability in the membrane potential (ΔV_n) we expect the resulting spike timing jitter will scale with, $\Delta t = \Delta V_n / \dot{V}$. Indeed, under noise stimulation, precise spike timing is observed (Bryant and Segundo 1976) with a timing precision that increases for faster stimuli (Mainen and Sejnowski, 1995). Corresponding simulations with a Hodgkin-Huxley neuron subject to membrane noise also show that increased stimulus magnitude increases timing precision (Schneidman 1998). A similar inverse dependence of spike time precision with stimulus intensity can be observed in cortical pyramidal neurons subject to synaptic noise (Shu et al. 2003). According to our theory, both a reduced time constant, as well as an increased magnitude of the stimulus, will increase membrane ramp slope and thus reduce timing jitter due to noise.

Functional Amplification – Network Consequences

We found that a 1 mV/mm uniform field induced in average a transmembrane potential change of ~ 0.1 mV. Compared to the scale of depolarization necessary to bring a neuron from rest to threshold (~ 15 mV), these fields were previously considered insignificant with respect to action potential initiation. Previous action potential threshold studies identified changes due to electric fields of less than 5 mV/mm (Jefferys et al., 1981). Rather than spike generation, here we demonstrated changes in timing, consistent with the proposed amplification mechanism.

The present results provide a potential mechanism for the effects on network spike timing previously demonstrated *in vitro* with exogenous uniform fields as low as 0.1 mV/mm (Deans et al., 2003; Francis et al., 2003; Fujisawa et al., 2004) and *in vivo* with calculated fields of 1.2 mV/mm (Marshall, 2006).

Electric field induced changes in spike timing would be particularly relevant for temporal coding during coherent (synchronous) network activity. For example, theta-modulated gamma activity in the hippocampus has been identified as a physiological correlate for a number of phenomena including spatial navigation, memory, etc. (Miller, 1991; Kahana et al., 2001; Canolty et al., 2006). Extracellular gamma activity amplitudes of up to 0.2 mV are observed *in vivo* (Csicsvari 2003) and *in vitro* (Hajos 2004, Mann 2004) with complete phase reversal across 100 μ m (from stratum pyramidale to stratum radiatum) resulting in field gradients of 4 mV/mm. An estimated gamma-field induced polarization of at least $\Delta V_e = 0.4$ mV (uniform field sensitivity providing a lower-bound for the coupling factor) is small compared to the full scale voltage fluctuations (e.g. AP threshold); however considering a theta oscillation synaptic ramp with slope of $\dot{V}_i = 0.2$ mV/ms (15 mV change between resting and firing potentials within 75 ms of a half a theta cycle), a time shift of $\Delta t = 1$ ms, and a Rayleigh vector strength of $r = 0.39$ with a mean angle of α , can be estimated. Thus extracellular fields oscillating at gamma frequency may have a functional effect on AP timing during theta activity even in a single cycle. Moreover, since gamma field activity is coherent across several mm of the pyramidal layer (Csicsvari et al., 2003; Mann et al., 2004), extracellular gamma oscillations could facilitate coherence across a large population of neurons. Finally, computational studies have demonstrated that an additional synchronizing effect may result during recurrent network activity when small changes in time add up over multiple cycles (Parra and Bikson, 2004).

The discussion above assumes that the timing of extracellular fields relative to synaptic input acts to promote coherent firing by advancing late spikes and delaying early spikes. However, a different temporal relationship between fields and underlying network activity could also have the opposite effect of advancing early spikes and delaying late spikes thus acting as a safety mechanism to prevent hyper-synchronization.

Our approach for predicting field-induced timing changes (Eq. 2, 3) can be readily extended to other networks using readily measurable extracellular and intracellular waveforms and using either field susceptibility estimates or our novel method to measure susceptibility. Indeed, extracellular field oscillations are a ubiquitous marker for network oscillations (Chrobak et al., 1998; Donoghue et al. 1998, Csicsvari, 2003; Nunez and Srinivasan, 2005; Sarnthein et al., 2007). More than an epiphenomenon, our results indicate a functional role for field potentials in modulating spike timing. Indeed, the information content of endogenous extracellular potentials oscillations is often comparable to multi-unit activity (e.g. Scherberger et al., 2005, Heldman and Wang, 2006, Liu and Newsome, 2006). Synaptic mechanisms underlie the generation of many classes of oscillations (Bragin et al., 1995; McBain et al. 1999; Buzsaki et al., 2003; Jones and Wilson, 2005; Siapas et al., 2005; Netoff et al., 2005); field-effect coupling is not proposed as alternative, but

rather as a complementary mechanism with unique spatio-temporal features.

Our system does not presuppose the source, exogenous or endogenous, of the modulating electric fields. Thus, the equations developed in this paper can be similarly applied in predicting the effects of environmental electric fields; EMF safety standards have not previously considered effects of timing. Finally, our results support the development of therapeutic stimulation technologies targeting neuronal timing; abnormal timing is indeed a hallmark of many neurological disorders and sub-threshold stimulation approaches may be readily adapted for non-invasive (transcranial) technologies.

Acknowledgment

Abhishek Datta of the City College of New York; Chris Leonard of New York Medical College; Denis Paré of Rutgers University; Jack Belgum, Adair Osterle, and Rick Ayer of Sutter Instruments; Tim Bergel and Simon Gray of Cambridge Electronic Design (CED). This work was supported in part by the Wallace H. Coulter Foundation and PSC-CUNY.

References

- Azouz R, Gray C.M. (2000) Dynamic spike threshold reveals a mechanism for synaptic coincidence detection in cortical neurons in vivo. *PNAS* 97(14):8110-8115
- Bikson M, Inoue M, Akiyama H, Deans JK, Fox JE, Miyakawa H, Jefferys JG (2004) Effects of uniform extracellular DC electric fields on excitability in rat hippocampal slices in vitro. *J Physiol.* 557(Pt 1):175-90.
- Bragin A, Jando G, Nadasdy Z, Hetke K, Wise K, Buzsáki G. (1995) Gamma (40-100 Hz) oscillation in the hippocampus of the behaving rat. *J. Neurosci* 15:47
- Bryant HL, Segundo JP (1976) Spike initiation by transmembrane current: a white-noise analysis. *J Physiol.* 260(2):279-314.
- Buzsáki G, Buhl DL, Harris KD, Csicsvari J, Czeh B, Morozov A. (2003) Hippocampal Network Patterns of Activity in the Mouse. *Neuroscience* 116:201
- Canolty RT, Edwards E, Dalal SS, Soltani M, Nagarajan SS, Kirsch HE, Berger MS, Barbaro NM, Knight RT (2006) High Gamma Power is Phase-Locked to theta Oscillations in Human Neocortex. *Science* 313:1625
- Chan CY, Nicholson C. J (1986) Modulation by applied electric fields of Purkinje and stellate cell activity in the isolated turtle cerebellum. *Physiol.* 371: 89-114.
- Chrobak JJ, Buzsáki G (1998) Gamma Oscillations in the Entorhinal Cortex of the Freely Behaving Rat. *J. Neurosci* 18:388
- Chrobak JJ, Lorincz A, Buzsáki G (2000) Physiological patterns in the hippocampo-entorhinal cortex system. *Hippocampus.* 10(4):457-65.
- Csicsvari J, Jamieson B, Wise KD, Buzsáki G. (2003) Mechanisms of gamma oscillations in the hippocampus of the behaving rat. *Neuron.* 37(2):311-22.
- de Ruyter van Steveninck RR, Lewen GD, Strong SP, Koberle R, Bialek W (1997) Reproducibility and variability in neural spike trains. *Science.* 275 (5307): 1805-8.
- Deans JK, Bikson M, Fox JE & Jefferys JGR (2003). Effects of AC fields at powerline frequencies on gamma oscillations in vitro. *Society for Neuroscience Annual Meeting* 258.1
- DeWeese MR, Wehr M, Zador AM (2003) Binary spiking in auditory cortex. *J Neurosci.* 23(21):7940-9.
- Donoghue JP, Sanes JN, Hatsopoulos NG, Gaál G (1998) Neural Discharge and Local Field Potential Oscillations in Primate Motor Cortex During Voluntary Movements. *J. Neurophysiology* 79, 159-173
- Durand DM, Bikson M (2001). Suppression and control of epileptiform activity by electrical stimulation: a review. *Proc IEEE* 89, 1065–1082
- Faber DS, Korn H. (1983) Field effects trigger post-anodal rebound excitation in vertebrate CNS. *Nature.* 305(5937):802-4
- Francis JT, Gluckman BJ, Schiff SJ (2003) Sensitivity of Neurons to Weak Electric Fields. *J. Neuroscience,* 23(19):7255-7261
- Fujisawa S, Matsuki N, Ikegaya Y. (2004) Chronometric readout from a memory trace: gamma-frequency field stimulation recruits timed recurrent activity in the rat CA3 network. *J. Physiol.* 561(1): 123-131
- Fischer Y, Wittner L, Freund TF, Gähwiler BH (2002) Simultaneous activation of gamma and theta network oscillations in rat hippocampal slice cultures. *J Physiol.* 539(Pt 3):857-68.
- Fricke D, Verheugen J, Miles R (1999). Cell-attached measurements of the firing threshold of rat hippocampal neurones. *J Physiol* 517.3, 791-804
- Ghai RS, Bikson M & Durand DM (2000). Effects of applied electric fields on low-calcium epileptiform activity in the CA1 region of rat hippocampal slices. *J Neurophysiol* 84, 274–280.
- Hajos N, Palhalmi J, Mann EO, Nemeth B, Paulsen O, Freund TF (2004) Spike timing of distinct types of GABAergic interneuron during hippocampal gamma oscillations in vitro. *J Neurosci.* 24(41):9127-37.
- Hamblin DL (2002) Effects of mobile phone emissions on human brain activity and sleep variables. *International Journal of Radiation Biology* 78(8):659-669
- Harris KD, Csicsvari J, Hirase H, Dragoi G, Buzsáki G (2003) Organization of cell assemblies in the hippocampus. *Nature* 424(6948):552-6.
- Harris K, Henze D, Hirase H, Leinekugel X, Dragoi G, Czurko A, Buzsáki G. (2002) Spike train dynamics predicts theta-related phase precession in hippocampal pyramidal cells. *Nature* 417:738-741
- Heldman DA, Wang W, Chan SS, Moran DW (2006) Local field potential spectral tuning in motor cortex during reaching. *IEEE Trans. Reh. Eng.* 14(2)
- Jefferys JG (1981) Influence of electric fields on the excitability of granule cells in guinea-pig hippocampal slices. *J Physiol.* 319:143-52.
- Jefferys JG, Deans J, Bikson M, Fox J. (2003) Effects of weak electric fields on the activity of neurons and neuronal networks. *Radiat Prot Dosimetry.* 106(4):321-3
- Jones M, Wilson M. (2005) Theta rhythms coordinate hippocampal-prefrontal interactions in a spatial memory task. *PLOS Biology* 3(12): e402
- Kahana M, Seelig J, Madsen JR. (2001) Theta Returns. *Curr. Opin. NeuroBiol.* 11:739
- Kara P, Reinagel P, Reid RC. (2000) Low response variability in simultaneously recorded retinal, thalamic, and cortical neurons. *Neuron.* (3):635-46.
- Kashiwadani H, Sasaki YF, Uchida N, Mori K. (1999) Synchronized oscillatory discharges of mitral/tufted cells with different molecular receptive ranges in the rabbit olfactory bulb. *J Neurophysiol.* 82(4):1786-92.
- Liu J, Newsome WT (2006) Local Field Potential in Cortical Area MT: Stimulus Tuning and Behavioral Correlations. *J. Neuroscience,* 26(30):7779-7790.
- Lutz A., Lachaux JP, Martinerie J, Varela F (2001) Guiding the study of brain dynamics by using first person data: Synchrony patterns correlate with ongoing conscious states during a simple visual task. *PNAS* 99(3):1586-1591
- Mainen ZF, Sejnowski TJ (1996) Influence of dendritic structure on firing pattern in model neocortical neurons. *Nature* 382(6589):363.

- Mainen ZF, Sejnowski TJ (1995) Reliability of spike timing in neocortical neurons. *Science*. 268(5216):1503-6.
- Mann EO, Radcliffe CA, Paulsen O. (2005) Hippocampal gamma-frequency oscillations: from interneurons to pyramidal cells, and back. *J Physiol*. 562(Pt 1):55-63.
- Marshall L, Helgadottir H, Molle M, Born J. (2006) Boosting slow oscillations during sleep potentiates memory. *Nature* 444(7119):610-3.
- Mehta MR, Lee AK, Wilson MA. (2002) Role of experience and oscillations in transforming a rate code into a temporal code. *Nature* 417(6890):741-6.
- Moore, D. S. and McCabe, G. P. (1999) Introduction to the Practice of Statistics, 3rd edition, New York: W. H. Freeman.
- McBain C, Freund T, Mody I. (1999) Glutamatergic synapses onto hippocampal interneurons: precision timing without lasting plasticity. *Trends in Neurosciences* 22(5):228-235
- McIntyre CC, Grill WM (1999) Excitation of central nervous system neurons by nonuniform electric fields. *Biophys J*. 76(2): 878-888.
- Miller R (1991) Cortico-hippocampal Interplay and the Representation of Contexts in the Brain. Springer-Verlag, New York
- Netoff T, Banks M, Dorval A, Acker C, Haas J, Kopell N, White J. (2005) Synchronization I Hybrid Neuronal Networks of the Hippocampal Formation. *J Neurophysiol*. 93:1197-1208
- Nunez PL, Srinivasan RS (2005) Electric Fields of the Brain: The Neurophysics of EEG. Oxford Univ. Press, Oxford
- Parra LC, Bikson M. (2004) Model of the effect of extracellular fields on spike time coherence, 26th Annual International Conference of the IEEE Engineering in Medicine and Biology Society 1 - 4
- Radman T, Parra LC, Bikson M. (2006) Amplification of small electric fields by neurons; implications for spike timing, 28th Annual International Conference of the IEEE Engineering in Medicine and Biology Society
- Rattay F. (1998) Analysis of the electrical excitation of CNS neurons. *IEEE Transactions on Biomedical Engineering* 45(6):766-772
- Riehle A, Grammont F, Diesmann M, Grun S. (2000) Dynamical changes and temporal precision of synchronized spiking activity in monkey motor cortex during movement preparation. *J Physiol Paris*. 94(5-6):569-82.
- Reinagel P, Reid RC. (2000) Temporal coding of visual information in the thalamus. *J Neurosci*. 20(14):5392-400.
- Sarnthein J., Jeanmonod D. (2007) High thalamocortical theta coherence in patients with Parkinson's disease. *J. Neurosci*. 27(1): 124-131
- Schaefer AT, Angelo K, Hartwig S, Margrie T (2006) Neuronal oscillations enhance stimulus discrimination by ensuring action potential precision *PLOS Biology* 4(6): 1010-24
- Scherberger H, Jarvis MR, Andersen RA (2005) Cortical local field potential encodes movement intentions in the posterior parietal cortex. *Neuron* 46: 347-354
- Schneidman E, Freedman B, Segev I. (1998) Ion channel stochasticity may be critical in determining the reliability and precision of spike timing. *Neural Computation* 10:1679-1703
- Shu Y, Hasenstaub A, Badoual M, Bal T, McCormick D.A. (2003) Barrages of Synaptic Activity Control the Gain and Sensitivity of Cortical Neurons. *J. Neurosci*. 23(32):10388-10401
- Siapas AG, Lubenov EV Wilson MA. (2005) Prefrontal Phase Locking to Hippocampal Theta Oscillations. *Neuron* 46:114
- Trussell LO. (1999) Synaptic mechanisms for coding timing in auditory neurons. *Annu Rev Physiol*. 61:477-96.
- Webster BR, Celnik PA, Cohen LG. (2006) Noninvasive brain stimulation in stroke rehabilitation. *NeuroRx*. 3(4):474-81

Supplementary section: Derivation of phase distribution for AC stimulation

In this experiment the membrane potential combines the injected current ramp plus the induced oscillatory polarization due to the applied extracellular field:

$$V(t) = V_i + \Delta V_E = t\dot{V}_i + cE \sin(\omega t) .$$

This can be written also in terms of phase, $\varphi = \omega t = 2\pi t / T$, within the oscillatory cycle:

$$V(\varphi) = \frac{\varphi}{2\pi} T\dot{V}_i + cE \sin(\varphi) .$$

The equations developed here are based on the threshold crossing mechanism commonly used as part of an integrate-and-fire model (see e.g. Gerstner and Kistler 2002). Assume that spike timing is determined entirely by the time at which the membrane potential reaches a fixed threshold. Cells only fire if they reach threshold from below ($\dot{V} > 0$). In addition, we only consider the first spike, and so the likelihood of a first spike is zero after the cell fired. Hence, there is zero probability of firing for all φ with a negative membrane slope, and for all φ with a membrane potential that is lower than some previous potential value. Call this set

$$S = \{ \varphi \mid dV / d\varphi < 0 \wedge V(\varphi) < V(\varphi'), \forall \varphi' < \varphi \} .$$

The likelihood of firing for those times is

$$p(\varphi) = 0 , \text{ for } \varphi \in S .$$

For all other times the likelihood of firing is determined by the likelihood that the membrane potential crosses the threshold value. Within a small time interval this likelihood of firing is therefore proportional to the increase in membrane potential (i.e. if the potential increase is large there is a high likelihood that threshold was crossed). Writing this in terms of phase gives:

$$p(\varphi) \propto \frac{dV}{d\varphi} , \text{ for } \varphi \notin S .$$

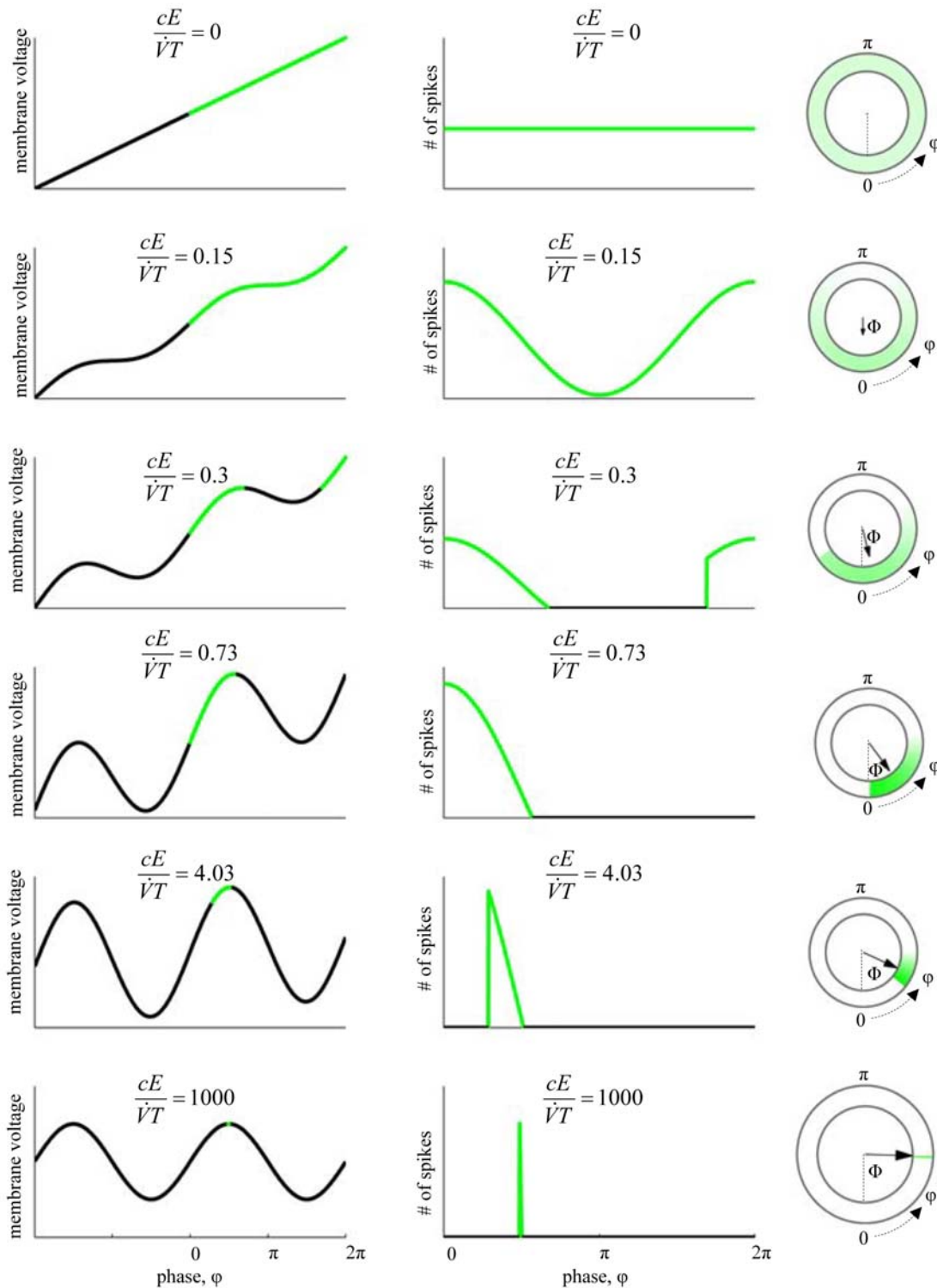
If the control condition without field application has (by virtue of intracellular stimulation) a non-uniform distribution of firing, $p_0(\varphi)$, then the overall likelihood of firing is weighted by that prior distribution. The value of the prior has to be evaluated for the phase that would have occurred without a field, i.e. $\varphi + \Delta\varphi$, with $\Delta\varphi = \frac{2\pi}{T} \frac{cE}{\dot{V}_i} \sin(\varphi)$. Combining everything this can be written as

$$p_E(\varphi) \propto p_0(\varphi + \Delta\varphi) \begin{cases} dV / d\varphi & \text{for } \varphi \notin S \\ 0 & \text{otherwise} \end{cases} = p_0(\varphi + \Delta\varphi) \begin{cases} \frac{T}{2\pi} + \frac{cE}{\dot{V}_i} \cos(\varphi) & \text{for } \varphi \notin S \\ 0 & \text{otherwise} \end{cases} .$$

The proportionality constant has to be chosen so that the distribution is properly normalized, i.e. $\int_{2\pi} d\varphi p(\varphi) = 1$. Equation 3 in the main text gives this result in a simplified form (assuming uniform $p_0(\varphi)$, and specifying the ranges for φ in words). It does include, however, an additional phase delay α . Assuming a passive membrane with first-order low-pass characteristics this phase delay relates to the membrane time constant as, $\tau = T \tan(\alpha)$.

Reference:

Gerstner W, Kistler W, Spiking Neuron Models, Cambridge University Press, 2002



Supplementary Figure S1. Theoretical predictions of spike timing phase response for a range of field-induced polarizations over voltage ramp slopes. Left column: Membrane voltage over two cycles with $cE(\dot{V}T)^{-1}$ ranging from 0 (no AC contribution) to 1000. The cell is constrained to fire within the range highlighted in green (see main text). Middle column: Predicted distribution of spike timing phase according to Eq. 3 (main). Right column: circular plot of phase distribution with mean angle and vector strength. The cell is constrained to fire in the green phase. The arrow direction shows the mean firing phase, Φ , relative to the extracellular field while arrow length represents vector strength, r . With increasing field strength coefficient, mean phase advances from 0 to $\pi/2$ and coherence increases. Note: The 5th row is that shown in the main text.